APPLIED GEOPHYSICS, Vol.12, No.2 (June 2015), P. 244-254, 14 Figures.
DOI: 10.1007/s11770-015-0482-4

Reservoir time-lapse variations and coda wave interferometry*

Tang Jie♦[1], Li Jing-Jing[1], Yao Zhen-An[1], Shao Jie[1], and Sun Cheng-Yu[1]

Abstract: Coda waves are multiply scattered waves that arrive much later than the major waves. Small seismic velocity variations are observed in reservoirs because of small variations in reservoir properties, which affect the first arrivals. Hence, first arrivals cannot be used to detect small seismic velocity variations. However, small variations can be reliably detected by the coda waves because of the amplification owing to multiple scattering. We investigate the ability of coda wave interferometry to detect seismic velocity variations and monitor time-lapse reservoir characteristics using numerical simulations and experimental data. We use the Marmousi II model and finite-difference methods to build model seismic data and introduce small seismic velocity variations in the target layer. We examine the model seismic data before and after the changes and observe the coda waves. We find that velocity changes can be detected by coda wave interferometry and demonstrate that coda wave interferometry can be used in monitoring time-lapse reservoir characteristics.
Keywords: time-lapse, coda wave, interferometry, wave velocity, scattering

Introduction

Coda means tail in Latin, and coda waves are part of the signal after the directly arriving phases (Aki,1969, 1985; Aki & Chouet, 1975). In the 1980s, Wu and Aki (1985) systematically investigated seismic wave scattering, including coda waves. Coda waves are multiply scattered during long-distance propagation and are sensitive to weak changes in the propagation medium (Kanu et al., 2014; An et al., 2015). Coda wave interferometry uses the differences before and after small disturbances to detect weak changes in propagation media. Presently, this method has been used to probe the relative location of seismic sources (Snieder and Vrijlandt, 2005; Sato, 1986; Robinson, 1987; Roberts et al., 1992; Qiao et al., 2014; Wang et al., 2010), to monitor rapid temporal changes in volcanoes (Grêt et al., 2005; Wegler, 2004; Ratdomopurdo and Poupinet, 1995), and applied to the time-lapse monitoring of rock properties in the laboratory (Grêt et al., 2006; Weaver and Lobkis, 2000). Snieder et al. (2002) used coda wave interferometry to obtain the signal delay and estimated the nonlinear seismic velocity variations. Coda wave interferometry was also used to detect spatially localized changes using single (Pacheco and Snieder, 2006)

Manuscript received by the Editor May 5, 2014; revised manuscript received April 22, 2015
*The research is sponsored by the 973 Program of China (No. 2013CB228604), the Natural Science Foundation of Shandong Province (No. ZR2013DQ020), the Fundamental Research Funds for the Central Universities (No.15CX08002A), and the National Natural Science Foundation of China (No. 41374123).
1. School of Geosciences, China University of Petroleum (East China), Qingdao 266580, China.
♦Corresponding author: Tang Jie (Email: tangjie@upc.edu.cn)

and multiple scattering (Pacheco and Snieder, 2005). Wang et al. (2008) collected seismic data in the Yunnan province and used coda wave interferometry to estimate changes in the seismic wave velocity. Song et al. (2012) conducted coda wave interferometry monitoring experiments to measure the elastic wave velocity change in rocks under stress. In addition, Ross et al. (1996) used seismic methods to monitor the time-varying characteristics of oil and gas layers and studied the time-lapse features of reservoirs. Lumley (2001) considered that time-lapse seismic monitoring could provide information about the fluid properties and pressure variations in the pore space of the reservoir. Recently, time-lapse seismic imaging has been used to monitor reservoir properties (Santos and Harris, 2007). Zhou et al. (2010) pointed that the accuracy of velocity data could affect the effectiveness of time-lapse monitoring.

The physical properties of oil and gas reservoirs change with time. These changes create differences in the seismic data over time within the same area. Hence, time-lapse seismic monitoring was developed. Ross et al. (1996) indicated that the ability to monitor reservoir changes as a function of time using seismic methods can improve the location of production and infill wells. Time-lapse seismic monitoring can provide information about changes in fluid properties in the reservoir pore spaces (Lumley, 2001). Time-lapse imaging has been successfully applied to reservoir monitoring in the oil industry (Santos and Harris, 2007). Nevertheless, these efforts are hampered by accuracy and precision limitations (Zhou et al., 2010).

Considering the accuracy of coda wave interferometry and the velocity precision requirements in time-lapse monitoring of reservoirs, we use coda wave interferometry to monitor time-lapse reservoir characteristics. We experimentally simulate the gradual saturation by fluids, and use numerical simulations and experiments to test the applicability of coda wave interferometry in reservoir time-lapse monitoring. Finally, we demonstrate that coda wave interferometry is a reliable and sensitive method to monitor time-lapse reservoir characteristics.

Coda wave interferometry

Snieder (2006) used coda wave interferometry to detect temporal changes in a propagation medium. In the following paragraphs, we briefly outline the method. Suppose that a strongly scattering medium is repeatedly excited by a source and the propagation medium characteristics change with time. When the propagation medium velocity changes over time, the dominant effect is the change t_P in the arrival times of the waves that propagate along different trajectories P, and the unperturbed wave field is

$$u_{unp}(t) = \sum_P A_P S(t - t_P). \tag{1}$$

Owing to scale differences in the propagation medium and the source wavelength, the wave encounters a large number of scatterers. Compared with a uniform propagation medium, these scatterers greatly increase the seismic propagation path. In equation (1), t_P is the travel time along path P, A_P is the coherent amplitude, $S(t)$ is source wavelet, and P is any possible scattering path.

When water or oil cause perturbations in the background velocity, the wave propagation delay time for path P is τ_P. Thus, the perturbed wave field is (Snieder, 2006)

$$\tilde{u}_{per}(t) = \sum_p A_p S(t - t_p - \tau_p). \tag{2}$$

If any reservoir property changes, there will be concomitant travel time perturbations during seismic wave propagation through the reservoir. The changes in the waveforms can be quantified by computing the time-shifted cross-correlation over a specific time window at time t with temporal width $2T$. The unperturbed and perturbed waves can be compared using the time-shifted correlation coefficient (Snieder, 2006)

$$R^{(t,T)}(t_s) = \frac{\int_{t-T}^{t+T} u_{unp}(t')\tilde{u}_{unp}(t'+t_s)dt'}{\sqrt{\int_{t-T}^{t+T} u_{unp}{}^2(t')dt \int_{t-T}^{t+T} \tilde{u}_{unp}{}^2(t')dt'}}, \tag{3}$$

where $u_{unp}(t)$ is the unperturbed wavefield, $\tilde{u}_{per}(t)$ is the perturbed wavefield and t_s is the time shift of the unperturbed and perturbed waves. t is the center of the finite time-window and $2T$ is the width of the window.

Inserting equations (1) and (2) into equation (3), we obtain the correlation coefficient (Snieder, 2006)

$$R^{(t,T)}(t_s) \approx \frac{\sum_{P(t,T)} A_P^2 C(\tau_p - t_s)}{\sum_{P(t,T)} A_P^2 C(0)}, \tag{4}$$

where the self-correlation of the source signal $C(t)$ is (Snieder, 2006)

$$C(t) \equiv \int_{-\infty}^{+\infty} S(t'+t)S(t')dt'. \tag{5}$$

Inserting the second-order Taylor expansion ($R_{\max} = 1 - \frac{1}{2}\overline{\omega^2}\,\sigma_\tau^{\,2}$) of equation (5) into equation (4), we obtain

$$R^{(t,T)}(t_s) = 1 - \frac{1}{2}\overline{\omega}^2 \left\langle (\tau - t_s)^2 \right\rangle_{(t,T)}, \qquad (6)$$

where $\overline{\omega}^2$ is the mean square frequency of the waves that arrive in the time window, and $\left\langle \cdots \right\rangle_{(t,T)}$ is the average over the wave paths with arrivals in the time interval $(t-T, t+T)$.

For maximun R_s, t_s

$$t_s = t_{\max} \equiv \left\langle \tau \right\rangle_{(t+T)}, \qquad (7)$$

where $\left\langle \tau \right\rangle_{(t+T)}$ is the mean travel time perturbation of the arrivals in the time window. Based on equations (6) and (7), the maximum correlation coefficient is

$$R_{\max} = 1 - \frac{1}{2}\overline{\omega^2}\,\sigma_\tau^{\,2}, \qquad (8)$$

where σ_τ^2 is the variance of the travel-time perturbation which is extracted from perturbation time of the waves that arrive at the time window, the time shift is given by the average perturbation of the travel time of waves that arrive at the specified time window. For each time interval, the time shift between the perturbed and unperturbed waves is determined by computing the time-shifted cross-correlation and by picking the time for which the cross-correlation coefficient is maximum at $t_{\max}$. The relative velocity change for each time interval is given (Snieder, 2002)

$$\frac{\delta v}{v} = -\frac{t_{\max}}{t}. \qquad (9)$$

The velocity change is a function of the central time t of the specified time window.

Experiment

Small changes in the propagation medium, which have no detectable effect on the first arrivals, are amplified because of multiple scattering and are readily seen in the coda waves. To validate the applicability of coda wave interferometry to reservoir monitoring, we perform experiments and numerical simulations.

Monitoring water saturation

A rock-velocity measuring system typically consists of a wave source, a receiver, and an oscilloscope, as shown in Figure 1a. The frequency of the probes is 1.5 MHz; thus, the sampling rate may reach up to 16 million per second. During the experiment, the sample is placed between the wave source and the receiver; the electronic signal passes through the sample and is then displayed on the computer screen.

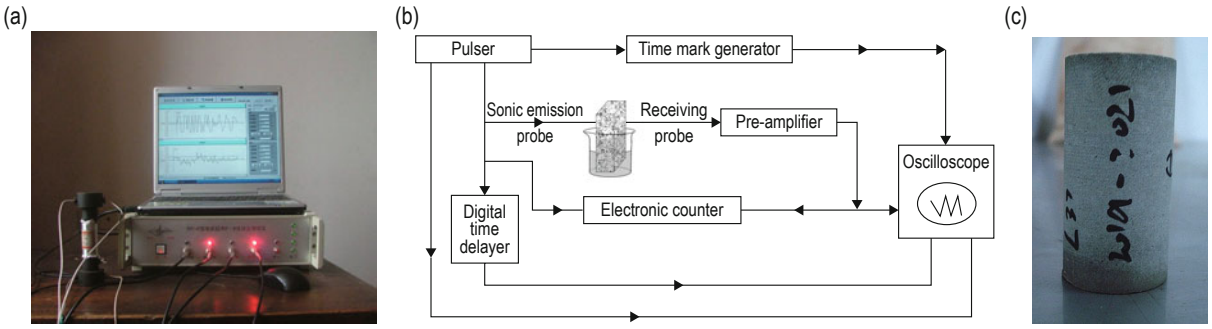

Fig.1 (a) Ultrasonic system; (b) sketch of the setup; (c) rock specimen.

We submerge a flat, room-dried sandstone specimen, as shown in Figure 1b, into a container with water. The water infiltrates the specimen via capillary absorption. We conduct ultrasonic measurements at specific water heights. Figure 2 shows two waveforms measured at different times and the corresponding water intrusion heights of 2 mm and 4 mm. The early arriving waves (upper panel) are unaffected by the saturation changes and cannot be used to monitor the weak changes in rock velocity caused by the saturation differences. The coda waves after the directly arriving phases (lower panel) show obvious decorrelation of the waveforms. Clearly, coda waves can be used to monitor the velocity changes owing to saturation differences.

As the propagation medium under investigation contains many small-scale scatterers and the waves

follow paths that connect the scatterers, the path of the scattered waves is much longer than that of the direct waves that move from the source to the receiver. Hence, the scattered waves are more sensitive to velocity changes than direct waves.

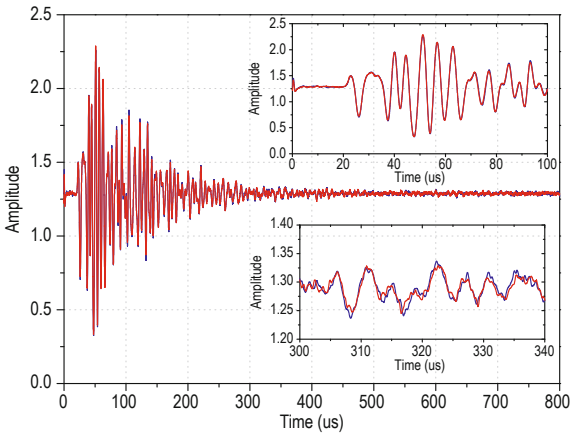

Fig.2 Waveforms at two different levels of water saturation; the water intrusion height is 2 mm and 4 mm, respectively.
The blue line represents early measurements and the red line represents late repeat measurements. The large background figure shows the entire waveforms. The upper panel shows the time window of the early measurements and the lower panel shows the time window of the late measurements (coda wave).

Rock saturation test

We use a water-saturated standard rock cylinder (Φ25 × 50 mm), as shown in Figure 1c, with smoothed upper and lower surfaces. During the experiment, we compress the specimen and the probes (1 MPa) axially for better specimen–probe coupling. Furthermore, we keep the experimental conditions constant. We let the specimen dry naturally and conduct ultrasonic measurements at different states of saturation and water heights. Then, we analyze the coda waveforms. The whole process lasts ten hours. Figure 3 shows two waveforms collected at two different times to show the changes in the waveforms with saturation. The initial waveforms do not differ, whereas the late do. As the positions of the source and receiver do not change, the only possibility is that the propagation medium has changed and this change is too weak to be detected by the direct waves. Coda waves carry information about the propagation medium, which can be used to infer the changes in sonic velocity owing to saturated changes. To quantitatively describe the differences in the waveforms, the cross-correlation coefficient of the direct and coda waves is calculated separately. The cross-correlation coefficient of the direct wave is about 0.99, whereas the coefficient of the follow-up waveform decreases to 0.96. This suggests that tiny changes in saturation are detected by the coda waves.

In the time window of the coda waves, the waves contain information about the travel-time disturbance. Coda wave interferometry can help us obtain information regarding the travel-time disturbance distribution by calculating the waveform cross-correlation. We show the relative velocity changes at different times in Figure 4. Coda waves are superimposed discontinuous scattered waves along different paths owing to structural inhomogeneities. Because coda waves are multiply scattered, whereas the primary waves reach the receiver directly, small seismic velocity variations are amplified as coda waves propagate. Naturally, the accuracy and sensitivity of coda wave interferometry are higher than methods based on one-way travel times. Obviously, with

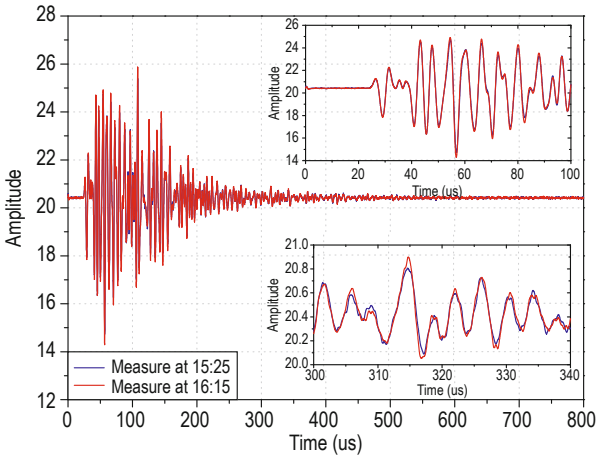

Fig.3 Waveforms in the sandstone sample at two different levels of water saturation.
The blue line represents the early measurements and the red line represents the repeat measurements. The large background figure shows the waveforms at different water saturation over time. The upper panel shows the time window of the early measurements and the lower panel shows the time window of the late measurements (coda).

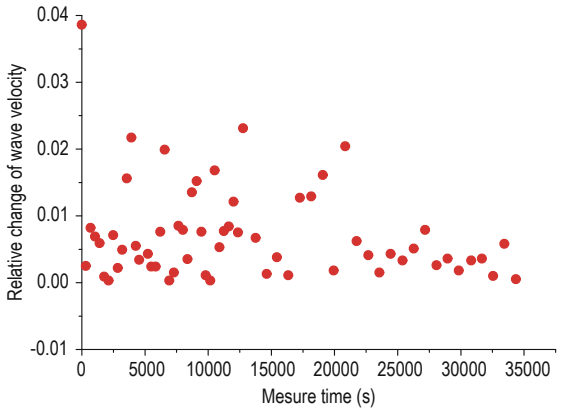

Fig.4 Relative velocity change dv/v in the sandstone specimen as a function of time.

coda wave interferometry, we can monitor small changes in wave velocity. This is difficult to do with primary waves.

Numerical simulation

We study the feasibility of coda wave interferometry for monitoring reservoir time-lapse characteristics using synthetic time-lapse data. The finite-difference method for solving the elastic wave equation is used to calculate synthetic seismograms of an explosive point source (Cheng, 1994).

Detection of small time-lapse velocity changes using coda wave interferometry

To investigate how to use coda wave interferometry to detect wave velocity perturbations and establish the smallest velocity changes, we use part of the Marmousi II model. We consider a 1625 m × 1500 m area with grid size of 1.25 m × 1.25 m, as shown in Figure 5a. The model velocity distribution is shown by the color bar and the red colored lenticular body represents a gas-bearing stratum. Assuming that the velocities of nonreservoir strata remain unchanged and the velocity in the reservoir changes slightly, coda wave interferometry is used to detect the velocity perturbations. In the following paragraphs, we analyze the time-lapse seismic monitoring using ground seismic and VSP data, respectively.

First, we calculate synthetic seismic data for reference. Then, we change the velocity values in the target layer (red layer in Figure 5a) and calculate the "test model" data. The test model data show 2% increase in the wave velocity. Numerical simulations with the unperturbed and test model for the lenticular body are performed based on the staggered-grid finite-difference method. In the numerical simulations, the source point is located at (812.5 m, 0 m), the number of traces is 1300, and the trace distance is 1.25 m. The seismic data are shown in Figures 5b and 5c, and it is obvious that small differences between unperturbed and perturbed seismic data cannot be readily identified.

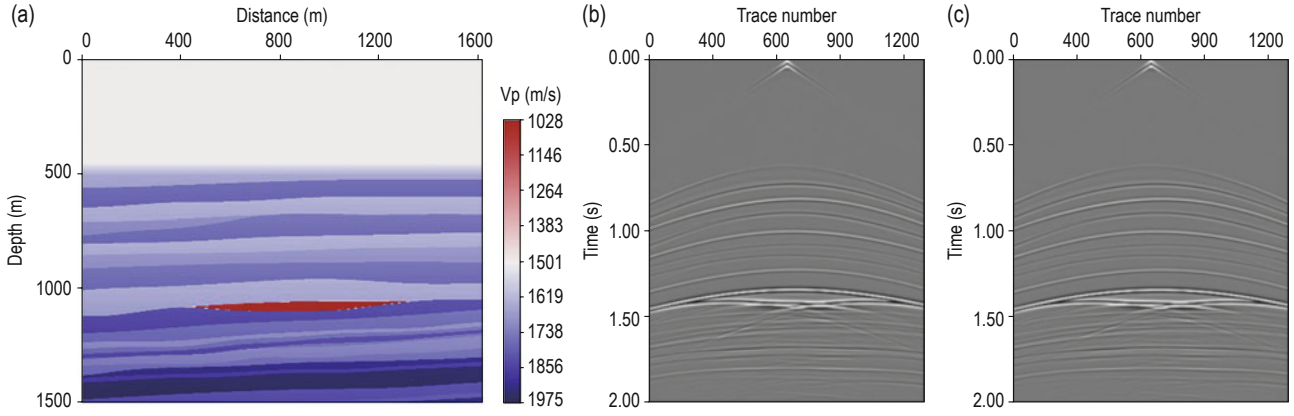

Fig.5 (a) Model sketch map (part of the Marmousi II model); seismic data for (b) reservoir velocity of 1028 m/s and (c) reservoir velocity 1048.7 m/s.

First, we compare the waveform for the 650th trace in the forward records. As shown in Figure 6a, to better compare them with the coda waves, only the 700–2000 ms segment is displayed. Figure 6a shows that there is almost no difference between the unperturbed seismic wave and the seismic wave with 2% velocity perturbation before 1300 ms. In contrast, the coda wave changes significantly. Therefore, slight velocity changes in reservoirs can be detected using coda waves but not head waves.

Second, to explore the effect of parameters, such as the temporal window length, coda wave interferometry is applied to the synthetic time-lapse data. The results indicate that a window length of about 1–2 wave periods contains fluctuations and includes outliers. When the window length is greater than three wave periods, the results of coda wave interferometry are almost the same. We calculate the temporal velocity changes at the centers of the moving time windows using coda wave interferometry and obtain the mean velocity change by averaging the temporal velocity changes over the entire time record.

Coda wave interferometry is also performed for the waves shown in Figure 6a. Figure 6b shows the starting

time of the finite time-windows on the horizontal axis and the time shift of the perturbed wave in the correlation in the vertical axis. The red dots in Figure 6b represent the average time shifts for the maximum correlation coefficient at different time-window lengths and the blue error bars are standard deviations. Figure 6b shows that the average time shift changes at about 1350 ms, which means that the velocity of model changes as well.

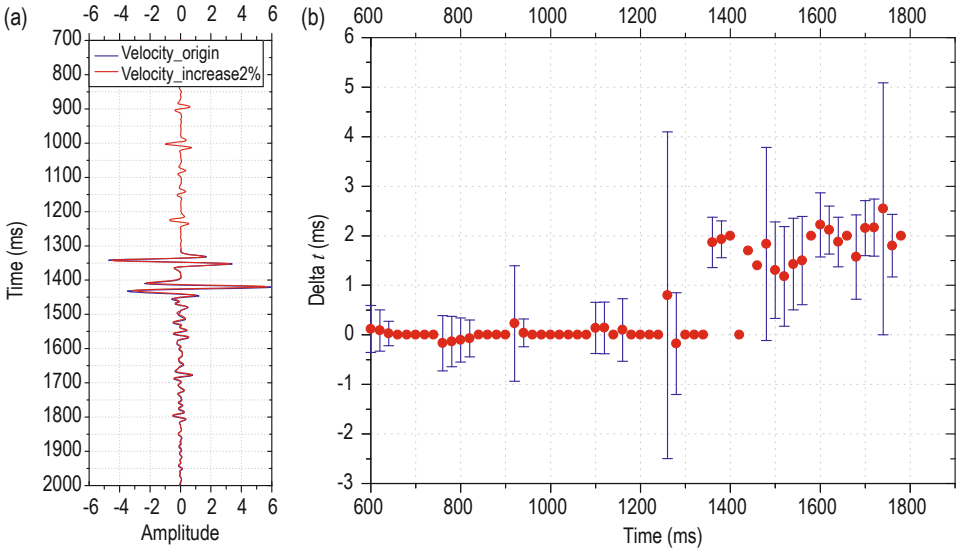

Fig.6 (a) Waveform comparison between unperturbed and 2% velocity perturbation seismic records; (b) coda wave interferometry with error bars for unperturbed and 2% velocity perturbation seismic record waves.

The time–depth conversion for the 650th trace record confirms the position corresponding to the time changes described above. According to the model, it is determined that for the 650th trace (x = 812.5 m), the top of the lenticular reservoir is at about 1058.75 m depth and the bottom is at about 1097.50 m. Figure 7 shows the theoretical relation between the wave propagation depth and zero-offset time for the 650th trace. The zero-offset time is calculated by superimposing the layer thickness/layer velocity of the 650th trace. Thus, we infer from Figure 7 that it takes the seismic wave about 1300 ms to arrive at top of the lenticular reservoir and 1400 ms to reach its bottom. In other words, the lenticular reservoir is at about 1300–1400 ms in the 650th trace record in the time domain. The average time shift changes at about 1350 ms in Figure 6b; thus, we confirm that coda wave interferometry can be used to detect slight velocity changes.

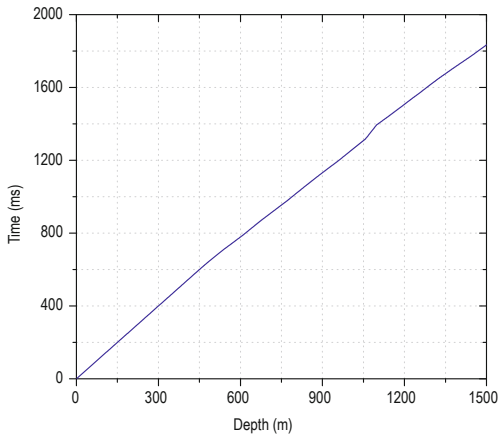

Fig.7 Time vs depth for the 650th trace record.

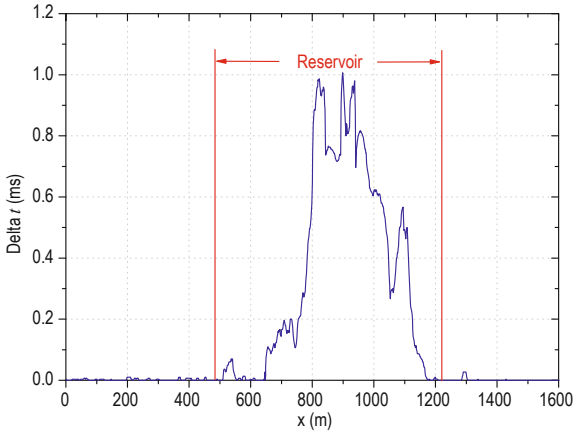

Fig.8 Time change Δt versus the receiver position for the time-lapse seismic data.

Coda wave interferometry can effectively detect small velocity variations in reservoirs. We average the estimated values over the entire seismic trace to obtain the mean Δt change for each receiver before and after the 2% change in reservoir velocity, and draw the Δt curve along with the change in the detector position in Figure 8. The latter shows the velocity change versus the receiver position in the time-lapse seismic data. The receivers with the maximum wave velocity changes are those near the target layer.

Coda wave interferometry of time-lapse VSP data

Based on forward modeling of the elastic wave equation, we obtain the VSP data using the model in Figure 5a. The source position is at (875 m, 0 m). There are 1001 sampling points in each trace and the sampling interval is 2 ms. Figure 9a shows the VSP data for the unperturbed and 2% velocity perturbation. The waveform comparison for the 700th trace in the forward records is shown in Figure 9b and it can be seen that there is almost no difference between the unperturbed VSP data and the VSP record with 2% velocity perturbation. Moreover, the coda wave interferometry for the unperturbed and 2% velocity perturbation VSP data is shown in Figure 9c. The red dots in Figure 9c represent the average time shift for the maximum correlation coefficient at different time-window lengths and the blue error bars are standard deviations of the average time shift. Obvious waveform changes are seen at about 800 ms in Figure 9c, which shows that the reservoir has also changed.

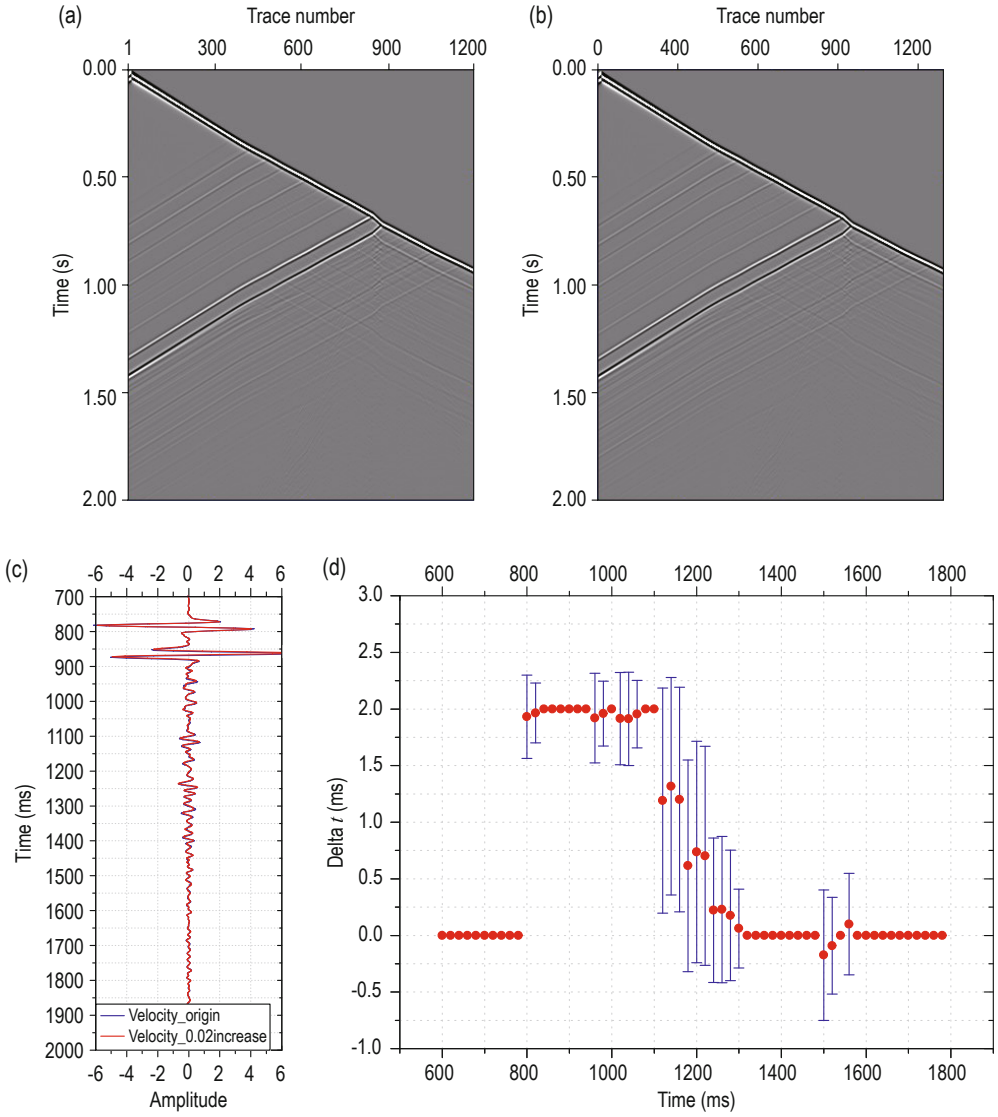

Fig.9 (a) VSP records; (b) waveform comparison of the unperturbed and 2% velocity perturbation VSP records; (c) coda wave interferometry with error bars for the unperturbed and 2% velocity perturbation VSP records.

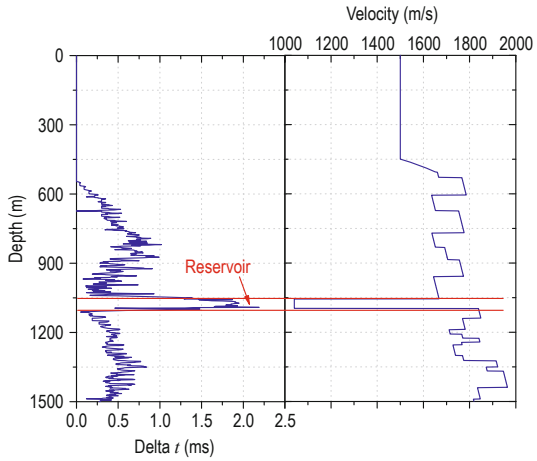

Fig.10 Time change Δt versus the receiver depth for the time-lapse VSP data.

We average the estimated values over the entire VSP trace to obtain the mean Δt change for each receiver before and after the 2% change in reservoir velocity. Figure 10 shows the velocity change versus the receiver depth for the time-lapse VSP data. At each receiver position, the waves have propagated through the target layer of which only a portion corresponds to the layer where the velocity change occurs. Therefore, the receivers with the maximum P-wave velocity changes are those near the target layer.

Smallest time-lapse velocity change detected using coda wave interferometry

Major velocity variations have an obvious effect on the travel time of head waves. Thus, it is unnecessary to amplify the velocity changes by coda wave interferometry. We analyze the detection capability of coda wave interferometry by numerical simulations. The simulations show that the monitoring capacity of coda waves is closely related to the source characteristics, sampling frequency, model parameters, and so on. To determine the smallest velocity perturbation that can be detected by coda wave interferometry, numerical simulations using the Marmousi II model for a lenticular reservoir are performed. The velocity is set to vary from 1% to 2% at 0.1% increments. We analyze specific traces (trace 650, zero-offset trace) and the velocity variations.

We only discuss the results for velocity differences of 1.2% and 1.3%. Figure 11a shows that it is impossible to detect the 1.2% velocity change using the head wave. Figure 11b shows that using coda wave interferometry we cannot detect the velocity change up to 1500 ms, which is inconsistent with the reflection time range of the reservoir response (almost between 1300 ms and 1400 ms). For the 1.3% velocity variation, it is still difficult to detect the velocity change with the head wave (Figure 12a), whereas coda wave interferometry (Figure 12b) can detect the velocity change at about 1350 ms. From the above analysis, we can conclude that the smallest velocity difference detected by coda wave interferometry is approximately 1.3%. A similar conclusion can also be drawn from Figures 13 and 14 based on the VSP data.

Coda wave interferometry gives a more global measure of velocity changes than transmitted waves. Based on sampling frequency and test data interpolation,

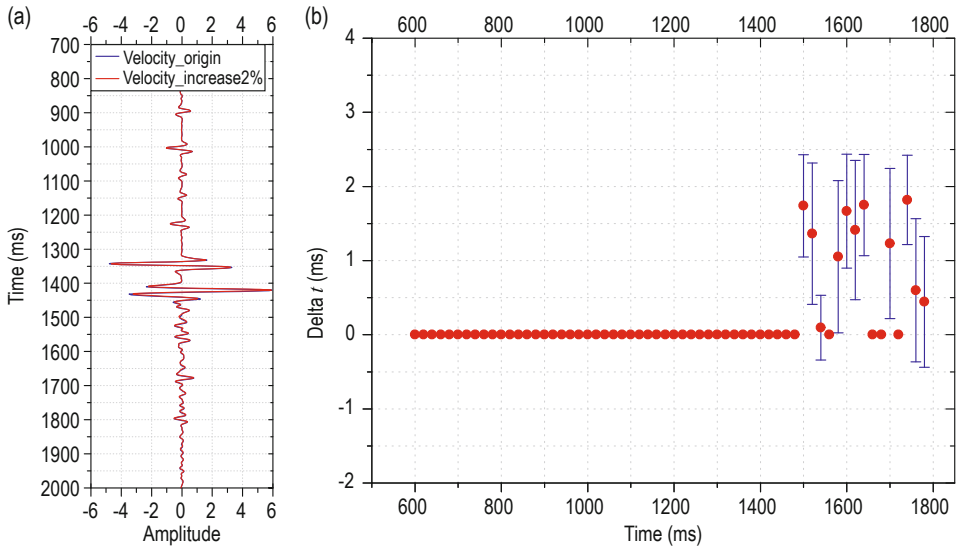

Fig.11 (a) Waveform comparison between unperturbed and 1.2% velocity perturbation seismic records; (b) coda wave interferometry with error bars for unperturbed and 1.2% velocity perturbation seismic records.

we may improve the monitoring precision; however, the monitoring sensitivity also depends on the signal-to-noise ratio and attenuation. In practice, this is not always possible because of instrument limitations, especially in the field, and attenuation (Chouet, 1979). Hence, it might not always be possible to record coda waves because the signal-to-noise ratio is too small or the attenuation too large.

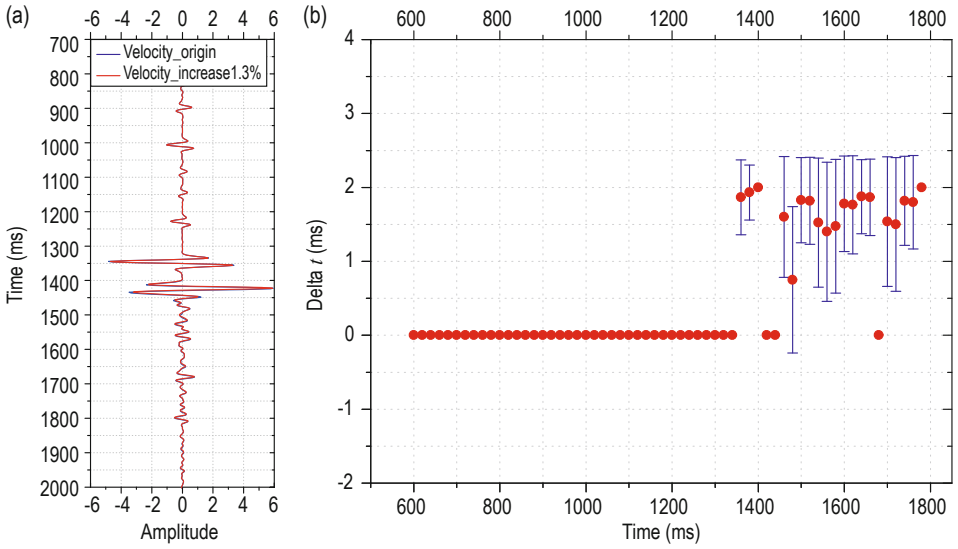

Fig.12 (a) Waveform comparison between unperturbed and 1.3% velocity perturbation seismic records; (b) coda wave interferometry with error bars for unperturbed and 1.3% velocity perturbation seismic records.

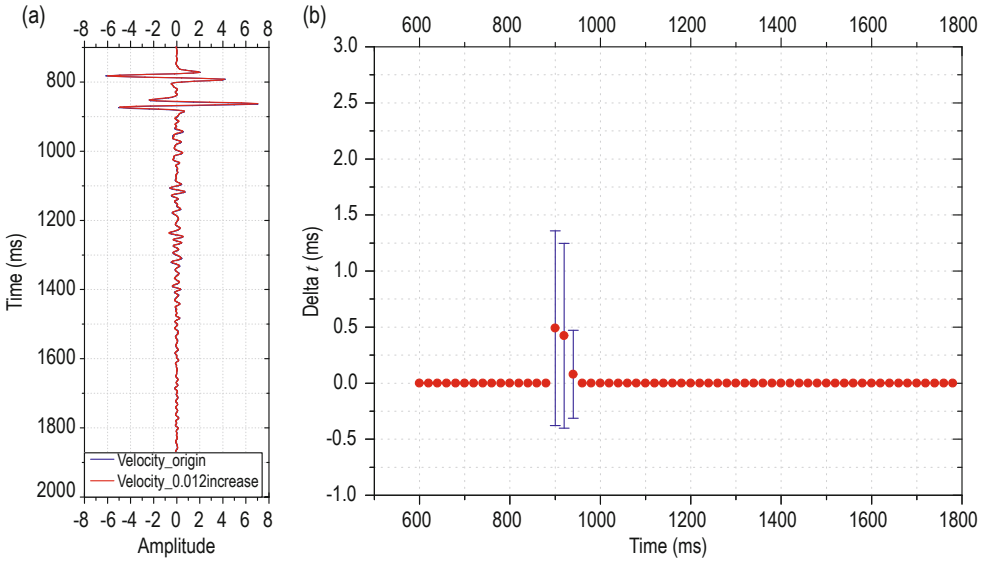

Fig.13 (a) Waveform comparison between unperturbed and 1.2% velocity perturbation VSP records; (b) coda wave interferometry with error bars for unperturbed and 1.2% velocity perturbation seismic records.

In this study, we mainly focused on the detection ability of coda wave interferometry. Previous work has shown that other methods, such as migration or inversion, can be used to obtain structural information and in time-lapse monitoring. Obviously, complete and high-quality seismic data are needed. Moreover, prestack inversion can be used to detect time-lapse attenuation. All these methods are different processing approaches of time-lapse seismic data.

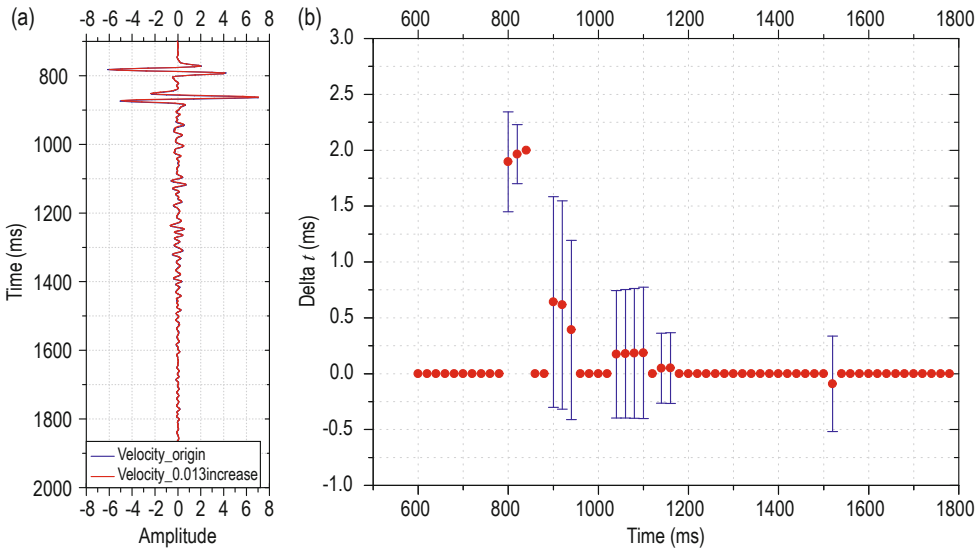

Fig.14 (a) Waveform comparison between unperturbed and 1.3% velocity perturbation VSP records; (b) coda wave interferometry with error bars for unperturbed and 1.3% velocity perturbation seismic records.

Conclusions

We can use coda waves to monitor pore fluid variations. We have investigated the application of coda wave interferometry to reservoir time-lapse monitoring. Numerical simulations and experimental data suggest that coda wave interferometry is a reliable method for reservoir time-lapse monitoring. Small reservoir velocity variations cannot be detected by head waves, whereas multiply scattered waves magnify these variations. Consequently, slight velocity changes can be observed. Coda wave interferometry can be used to monitor minor changes in reservoir properties, to enhance the efficiency and accuracy of time-lapse seismic reservoir monitoring, and to improve field production. Data repeatability affects monitoring; thus, in the future we will examine time-lapse data with inconsistent acquisition geometries.

References

Aki, K., 1969, Analysis of the seismic coda of local earthquakes as scattered wave: Journal of Geophysical Research, **74**(2), 615–631.

Aki, K., and Chouet, B., 1975, Origin of coda waves: Source, attenuation, and scattering effects: Journal of Geophysical Research, **80**(23), 3322–3342.

Aki, K., 1985, Theory of earthquake prediction with special reference to monitoring of the quality factor of lithosphere by the coda method: Practical Approaches to Earthquake Prediction and Warning, Springer Netherlands, 219–230.

An S. P., Hu T. Y., Cui, Y. F., Duan, W. S., and Peng, G. X., 2015, Auto-pick first breaks with complex raypaths for undulate surface conditions: Applied Geophysics, **12**(1), 93–100.

Cheng, N., 1994, Borehole wave propagation in isotropic and anisotropic media: three-dimension finite difference approach: PhD Thesis, Massachusetts Institute of Technology.

Chouet, B., 1979, Temporal variation in the attenuation of earthquake coda near Stone Canyon, California: Geophysical Research Letters, **6**(3), 143–146.

Grêt, A., Snieder, R., Aster, R. C., and Kyle, P. R., 2005, Monitoring rapid temporal change in a volcano with coda wave interferometry: Geophysical Research Letters, **32**(6).

Grêt, A., Snieder, R., and Scales, J., 2006, Time-lapse monitoring of rock properties with coda wave interferometry: Journal of Geophysical Research: Solid Earth (1978–2012), **111**(B3).

Kanu, C., Snieder, R., and Pankow, C., 2014. Time-lapse monitoring of velocity changes in Utah, Journal Geophysics Research Solid Earth, **119**, (9), 7209–7225.

Lumley, D. E., 2001, Time-lapse seismic reservoir monitoring: Geophysics, **66**(1), 50–53.

Pacheco, C., and Snieder, R., 2005, Time-lapse travel time change of multiply scattered acoustic waves: The Journal of the Acoustical Society of America, **118**(3), 1300–1310.

Pacheco, C., and Snieder, R., 2006, Time-lapse travel time change of singly scattered acoustic waves: Geophysical Journal International, **165**(2), 485–500.

Qiao, B. P., Guo P., Wang, P., and Hu, T. Y., 2014, Effectively picking weak seismic signal near the surface based on reverse virtual refraction interferometry. Chinese Journal Geophysics, **57**(6), 1900–1909.

Ratdomopurbo, A., and Poupinet, G., 1995, Monitoring a temporal change of seismic velocity in a volcano: Application to the 1992 eruption of Mt. Merapi (Indonesia): Geophysical Research Letters, **22**(7), 775–778.

Roberts, P. M, Phillips, W. S., and Fehler, M. C., 1992, Development of the active doublet method for measuring small velocity and attenuation changes in solids: The Journal of the Acoustical Society of America, **91**(6), 3291–3302.

Robinson, R., 1987, Temporal variations in coda duration of local earthquakes in the Wellington region, New Zealand: Pure and Applied Geophysics, **125**(4), 579–596.

Ross, C. P., Cunningham, G. B., and Weber, D. P., 1996, Inside the crossequalization black box: The Leading Edge, **15**(11), 1233–1240.

Santos, E. T. F., and Harris, J. M., 2007, Time-lapse diffraction tomography for trigonal meshes with temporal data integration applied to CO2 sequestration monitoring: 77th Ann. Internat. Mtg, Soc. Expl. Geophys., Expanded Abstracts. **26**, 2959–2963.

Sato, H., 1986, Temporal change in attenuation intensity before and after the eastern Yamanashi earthquake of 1983 in Central Japan: Journal of Geophysical Research: Solid Earth (1978–2012), **91**(B2), 2049–2061.

Snieder, R., 2006, The theory of coda wave interferometry: Pure and Applied Geophysics, **163**(2-3), 455–473.

Snieder, R., Greˆt, A., Douma, H., and Scales, J., 2002, Coda wave interferometry for estimating nonlinear behavior in seismic velocity: Science, **295**(5563), 2253–2255.

Snieder, R., and Vrijlandt, M., 2005, Constraining relative source locations with coda wave interferometry: Theory and application to earthquake doublets in the Hayward Fault, California: AGU Fall Meeting Abstracts, **1**, 1020.

Song, L. L., Ge, H. K., Guo, Z. W., and Wang, X. Q., 2012, Experimental study on the variation of media properties monitoring using multiple scattering waves: Chinese Journal of Rock Mechanics and Engineering, **31**(4), 713–722.

Wang, B. L., Zhu, G. M., and Gao, J. H., 2010, Joint interferometric imaging of walkaway VSP data: Applied Geophysics, **6**(1), 41–48.

Wang, B. S., Zhu, P., Chen, Y., Niu, F., and Wang, B., 2008, Continuous subsurface velocity measurement with coda wave interferometry: Journal of Geophysical Research, **113**(B12).

Weaver, R. L., and Lobkis, O. I., 2000, Temperature dependence of diffuse field phase: Ultrasonics, **38**(1), 491–494.

Wegler, U., 2004, Diffusion of seismic waves in a thick layer: Theory and application to Vesuvius volcano: Journal of Geophysical Research, **109**(B7).

Wu, R. S., and Aki, K., 1985, Scattering characteristics of elastic waves by an elastic heterogeneity: Geophysics, **50**(4), 582–595.

Zhou, R. M., Huang, L. J., Rutledge, J. T., Fehler, M., and Daley, T. M., 2010, Coda-wave interferometry analysis of time-lapse VSP data for monitoring geological carbon sequestration: International Journal of Greenhouse Gas Control, **4**(4), 679–686.

Tang Jie received his Ph.D. in Geophysics from the University of Science and Technology of China. He is presently at the College of Geosciences, China University of Petroleum. His research interests are seismic rock physics and seismic wave modeling.